Effect of El Niño on the mesosphere/lower thermosphere winds over Collm (51.3°N, 13°E)

Jacobi, Ch.[+], Mewes, D. [+], Ermakova, T.*, Pogoreltsev, A.I.*

+) Institute for Meteorology, Universität Leipzig, Stephanstr. 3, 04103 Leipzig, E-Mail: jacobi@uni-leipzig.de
**) Russian State Hydrometeorological University, St. Petersburg, Russia*

Summary: Mesosphere/lower thermosphere (MLT) zonal winds measured by a VHF meteor radar at Collm, Germany (51.3°N, 13.0°E) during late winter 2015/2016 show very strong westerly winds above about 90 km, but not below that height. This anomaly appears during a very strong El Niño event. The comparison of Niño3 equatorial sea surface temperature index and the Collm MLT wind time series starting in 2004 shows that in January and especially in February zonal winds are positively correlated with the Niño3 index. The signal is strong for the upper altitudes (above 90 km) accessible to the radar observations, but weakens with decreasing height. This reflects the fact that during El Niño years the westerly winter middle atmosphere wind jet is weaker on an average, and this is also the case with the easterly lower thermospheric jet. The El Niño effect on the meridional wind is weak. The experimental results can be qualitatively reproduced by numerical experiments using the MUAM mechanistic global circulation model with prescribed tropospheric temperatures and latent heat release for El Niño and La Niña conditions.

Zusammenfassung: Der Zonalwind in der oberen Mesosphäre/unteren Thermosphäre über Collm (51.3°N, 13.0°E) in der zweiten Hälfte des Winter 2015/2016 weist eine besonders starke westliche Komponente oberhalb von etwa 90 km auf. Diese Anomalie erfolgte während eines sehr starken El Niño-Ereignisses. Der Vergleich von Collmer Zonalwinden seit 2004 und dem Niño3-index zeigt im Januar und besonders Februar eine positive Korrelation. Diese ist stark oberhalb von 90 km, nimmt aber nach unten hin ab. Dies spiegelt die Tatsache wider, dass während El Niño-Jahren im Mittel der stratosphärische/mesosphärische Westwindjet schwächer ist. Dieses Signal kehrt aber in der oberen Mesosphäre um, so dass der thermosphärische Ostwindjet ebenfalls schwächer ist. Der Effekt auf den meridionalen Wind ist schwächer. Die Beobachtungen können mit Modellexperimenten qualitativ reproduziert werden.

1. Introduction

Mesosphere/lower thermosphere (MLT) winds and temperatures show considerable variability at time scales of several years, which is at least partly owing to the influence of atmospheric variability below. One of the primary circulation patterns at equatorial latitudes, which also affects climate worldwide is El Niño and its counterpart La Niña. El Niño events are characterised by high central Pacific sea surface temperature (SST), more clouds over the Pacific, and an anomaly of the Walker circulation. They are also connected with a cooling of the equatorial stratosphere and therefore a reduced temperature gradient between lower latitudes and the polar vortex and weakening of the latter. For El Niño years, there is also enhanced probability of sudden stratospheric warmings, which have effect on the North Atlantic and Eurasian troposphere (Camp and Tung, 2007; Polvani et al., 2017). On an average the polar stratospheric vortex is weaker during El Niño years than it is during La Niña years. This means that the high-latitude stratosphere is warmer during El Niño years, however, the mesosphere is colder then, which has been also observed by satellites and could also successfully been modelled (Garcia-Herrera et al., 2006; Fischer et al., 2008; Lu et al., 2011; Li et al., 2013).

There has been considerable interest in a possible coupling of El Niño also with the MLT region. Jacobi and Kürschner (2002) found that the correlation between El Niño and zonal wind at 90 km altitude over Collm, Germany (51.3°N, 13°E), is mainly negative in winter, but weakly positive in summer. They used data from 1979 – 1999. However, Jacobi (2009), using the same dataset extended until 2008 showed that after the 1990s these correlations decrease and even tend to reverse.

Modelling of El Niño influence on the middle atmosphere has mainly been done with focus on the temperature response and wave forcing. From WACCM model runs Li et al. (2013) obtained negative (westward) wave drag in the stratosphere during El Niño, but positive drag in the mesosphere. Consequently this is connected with easterly wind anomalies in the stratosphere, as reported by Taguchi and Hartmann (2006), Fischer et al. (2008) and Lu et al. (2011). The positive wave drag anomaly in the mesosphere reduces this negative wind anomaly. Most models, however, are confined to the stratosphere and mesosphere, or the analyses for the MLT did not focus on the wind.

Here we use observations at Collm made with a VHF meteor radar since 2004, which, in contrast to the earlier analyses by Jacobi and Kürschner (2002) and Jacobi (2009) cover the entire height region between about 80 and 100 km. We also apply the Middle and Upper Atmosphere Model (MUAM), which is a mechanistic circulation model from the ground to the thermosphere to interpret the observations.

2. Collm MLT wind measurements

At Collm Observatory (51.3°N, 13°E), a SKiYMET meteor radar is operated on 36.2 MHz since summer 2004 (Jacobi, 2012). The wind measurement principle is the detection of the Doppler shift of the reflected VHF radio waves from ionised meteor trails, which delivers radial wind velocities at the position of the meteor. An interferometer, consisting of five 2-element Yagi antennas arranged as an asymmetric cross was used to detect azimuth and elevation angle from phase comparisons of individual receiver antenna pairs. Together with range measurements the meteor trail position can be de-

tected. The raw data collected consist of azimuth and elevation angle, wind velocity along the line of sight from the receiving antenna to the meteor, meteor height, and additionally the decay time for each single meteor trail. The data collection procedure is also described in detail by Hocking et al. (2001). Recently, the Collm radar system has been upgraded, and the main modifications are higher power and the use of a 4 element transmitting antenna. This effectively increases the number of observed meteors and consequently the height range of wind measurements. The wind analyses, however, are not affected because they rely only on the Doppler shift of the reflected radio waves, and not on meteor parameters.

The individual meteor trail reflection heights roughly vary between 75 and 110 km, with a maximum around 90 km (e.g. Stober et al., 2008). In the standard configuration used here, the data are binned in 6 different not overlapping height gates centred at 82, 85, 88, 91, 94, and 98 km. Individual winds calculated from the meteors are collected to form half-hourly mean values using a least squares fit of the horizontal wind components to the raw data under the assumption that vertical winds are small (Hocking et al., 2001). An outlier rejection is added. Note that the nominal heights not necessarily correspond to the mean heights within the gates, because the meteors show a vertical distribution with increasing/decreasing count rates with height below/above about 90 km (Stober et al., 2008; Jacobi, 2012). Therefore, below/above 90 km mean heights tend to be higher/lower than nominal heights, and due to the small number of meteors at high altitudes, a substantial difference is visible for 98 km nominal altitude, so that the real mean height is closer to 97 km than 98 km (Jacobi, 2012). For the other height gates, the difference between real and nominal height may be neglected.

Time series of monthly mean wind parameters have been calculated applying a least-squares regression analysis of either zonal or meridional half-hourly horizontal winds collected during one month each on a model wind field including mean wind, diurnal, semidiurnal and terdiurnal oscillation. The results have been attributed to the centre of the respective time interval, and the analysis was repeated for each month. The 2005 – 2015 mean seasonal cycles of the zonal and meridional mean wind at 94 km and 85 km are shown in Fig. 1. The standard deviations of the monthly means are added as error bars, while the single monthly means are shown as small asterisks. The seasonal cycles are similar to those reported earlier e.g. by Jacobi (2012). The zonal winds show the uppermost part of the westerly wind jet in winter. In spring/summer the upper part of the easterly mesospheric wind jet is visible, while at 94 km the lower thermospheric westerly jet can be seen. The wind reversal is connected with the meridional southward jet.

In Fig. 1, the monthly mean winds for December 2015, January 2016 and February 2016 are highlighted. The January and February 2016 zonal winds at 94 km are the strongest that has been observed so far. However, this is not the case at 85 km. The meridional winds do not show a specific behaviour during this winter. The 2015/2016 winter was characterised by a strong El Niño event (Kennedy et al., 2016) which, among others, contributed to the extremely high Arctic temperatures this winter (Cullather et al., 2016). Therefore we assume that the strong MLT winds are connected with El Niño, and analyse this based on the Collm radar observations and numerical modelling in the following.

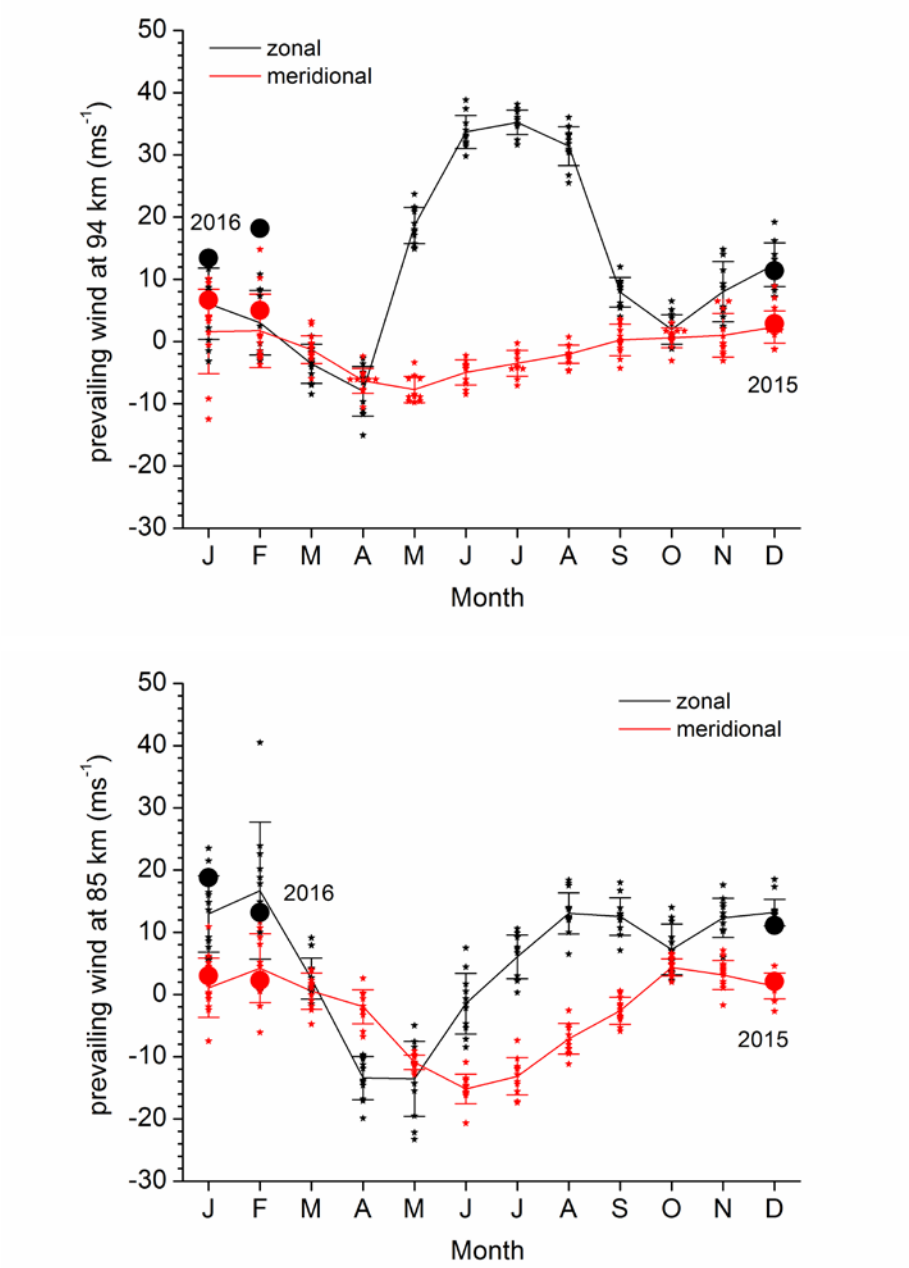

Fig. 1: 08/2004 – 04/2016 mean monthly mean zonal (black) and meridional (red) mean winds over Collm at 94 km (upper panel) and 85 km (lower panel). Error bars show the standard deviation of the monthly means, single months are added as small asterisks. Winter 2015/16 values are highlighted as big circles.

3. Correlation of Collm zonal winds and El Niño

To compare the variability of MLT zonal winds with El Niño, we use the Niño3 index, which represents the normalized area averaged SST in the region from 5°S-5°N and 150°W-90°W. We use SST from NOAA Extended Reconstructed Sea Surface Temperature (ERSSTA, Huang et al., 2015), Version 4, normalized to 1981-2010 (KNMI, 2016). There are several indices available that can be used for definition of El Niño (e.g. Trenberth, 1997). The Niño3 index represents the sea surface temperature in the

eastern part of the Pacific. The different indices are strongly correlated and the results should not differ qualitatively if another index would be used.

Correlation coefficients of monthly mean Niño3 index and MLT wind at different altitudes were calculated for each month and each radar altitude gate, and the results are shown in Fig. 2. The strongest El Niño response is seen for the zonal wind in February for the upper height gates. The effect decreases with decreasing altitude and even reverses for the lowest height gates. During the other months of the year the correlation is weaker. The results for winter are in correspondence with literature results. The middle atmosphere zonal winds during El Niño are weakened, but the positive wave drag in the mesosphere reduces this effect with increasing altitude, and eventually will lead to the reversal that can be observed in the Collm measurements. For the meridional wind component (lower panel of Fig. 2) the correlation is weaker and not significant.

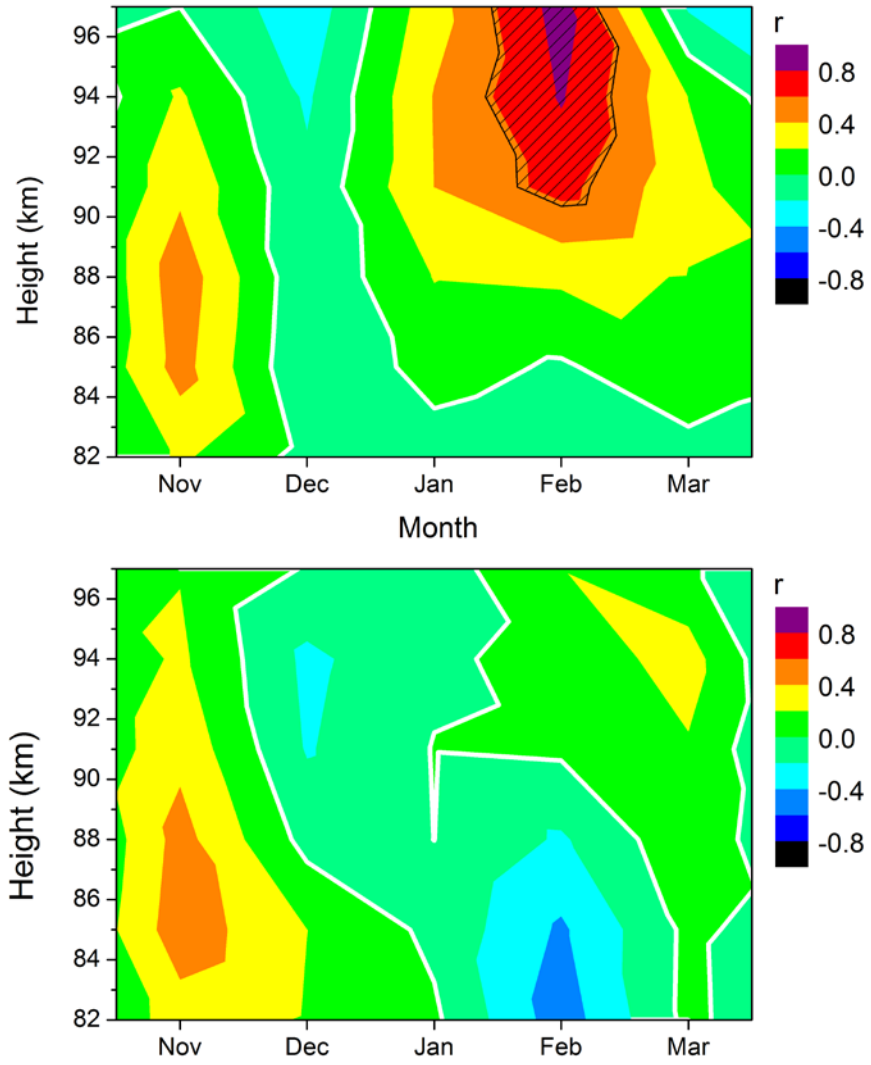

Fig. 2: Correlation coefficients of monthly mean zonal (upper panel) and meridional (lower panel) winds at different heights and Niño3 indices. Data from 08/2004 – 07/2016 have been used. Significant values at the 5% level according to a t-test are hatched.

4. Numerical model results

In order to substantiate the observed correlation of zonal winds with El Niño, we use MUAM model to simulate the MLT response to El Niño. MUAM is a nonlinear primitive equation 3D grid point mechanistic model with a resolution of 5°x5.625° in the horizontal and 56 vertical layers expressed in log-pressure height $z = -H \cdot \ln(p/p_0)$ with a constant scale height H = 7 km and p_0 = 1000 hPa. The vertical layers are spaced evenly with a step size $\Delta z = 0.4 \cdot H$. Further details can be obtained from Pogoreltsev et al. (2007).

Heating of the atmosphere due to absorption of solar radiation by water vapor, CO_2, ozone, oxygen and nitrogen is introduced in the model (Fröhlich et al., 2003). Infrared cooling of CO_2 is parameterized after Fomichev et al. (1998), while ozone infrared cooling in the 9.6 μm band is calculated after Fomichev and Shved (1985). Gravity waves in the middle atmosphere are parameterized based on an updated linear scheme (Fröhlich et al., 2003).

To consider the El Niño influence on the dynamical processes in the extra-tropical middle atmosphere, a semi-empirical parameterization of the latent heat release has been included that takes into account diurnal and longitudinal variations. Latent heating composites for Northern Hemisphere January under El Niño and La Niña conditions have been calculated using MERRA (Rienecker et al., 2011) reanalysis precipitation data. The corresponding composites of geopotential height and temperature at the lower boundary have been constructed from JRA-55 (Kobayashi et al., 2015) reanalyses. The El Niño and La Niña composites have been constructed from 9 strong or moderate events each. The January 2010 fields thus were included in the El Niño composite, but not January 2007. The recent 2015/16 El Niño also has not been included so that only one El Niño event was both included in the composite and covered by the observations. Regarding La Niña, January 2008 and January 2011 fields have been included in the composite, and 7 more cases that for earlier years when radar observations were not available. We therefore expect that, while the overall behaviour of zonal winds in our observations might be reproduced by the model, there will be differences in detail. Ensemble runs consisting of 10 members for El-Niño and La-Niña conditions, respectively, have been performed and ensemble means and their standard deviations have been calculated. The following results have been also presented in Jacobi et al. (2017).

We performed model runs for January conditions. Niño3 sea surface temperatures during the El Niño events peaked near the end of the years 2006, 2008, and 2015, while the zonal wind maximises in January or February of the following year, so that there is a delay in MLT response to El Niño. However, with MUAM we are modelling quasi-stationary cases, so that using January conditions represents a compromise between the delayed response and the stationary modelling approach.

January mean zonal mean latitude-log-pressure height cross-sections of temperature and zonal wind as simulated with MUAM for El Niño conditions are shown in Fig. 3. The latitude-height structure reproduces observed features known e.g. from empirical climatologies like URAP (Swinbank and Ortland, 2003,) or the radar based GEWM (Portnyagin et al., 2004). At 50-55°N there is a wind reversal from the mesospheric

westerly jet to the lower thermosphere easterly jet at about 90 km, which is a little bit lower than observed.

The mean differences between El Niño and La Niña years are shown in Fig. 4. The temperatures on the left panel show the stratospheric warming and mesospheric cooling during El Niño years known from global observations and other models (Garcia-Herrera et al., 2006; Li et al., 2013). The reduced stratospheric wind jet reported in the literature (Taguchi and Hartmann, 2006; Fischer et al., 2008; Lu et al., 2011) is shown in the right panel of Fig. 4, and above that in the MLT an increase of the zonal wind is visible. This qualitatively reproduces the Collm observations.

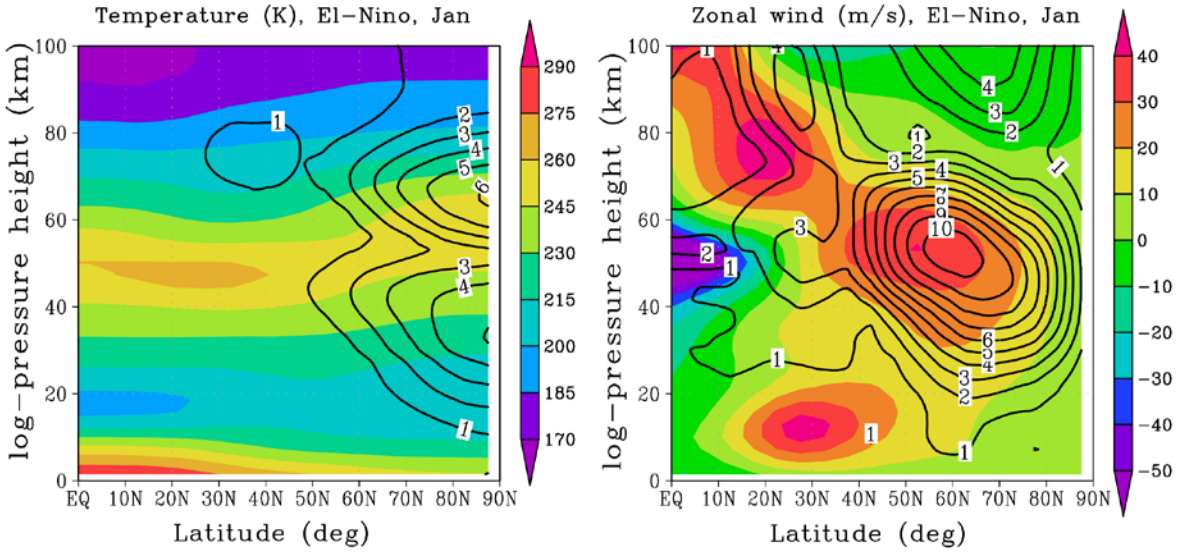

Fig. 3: January mean temperatures (left) and zonal winds (right) as simulated with MUAM for El Niño conditions. Colour coding shows mean values over 10 ensemble runs. Standard deviations of the ensemble members are added as black contour lines.

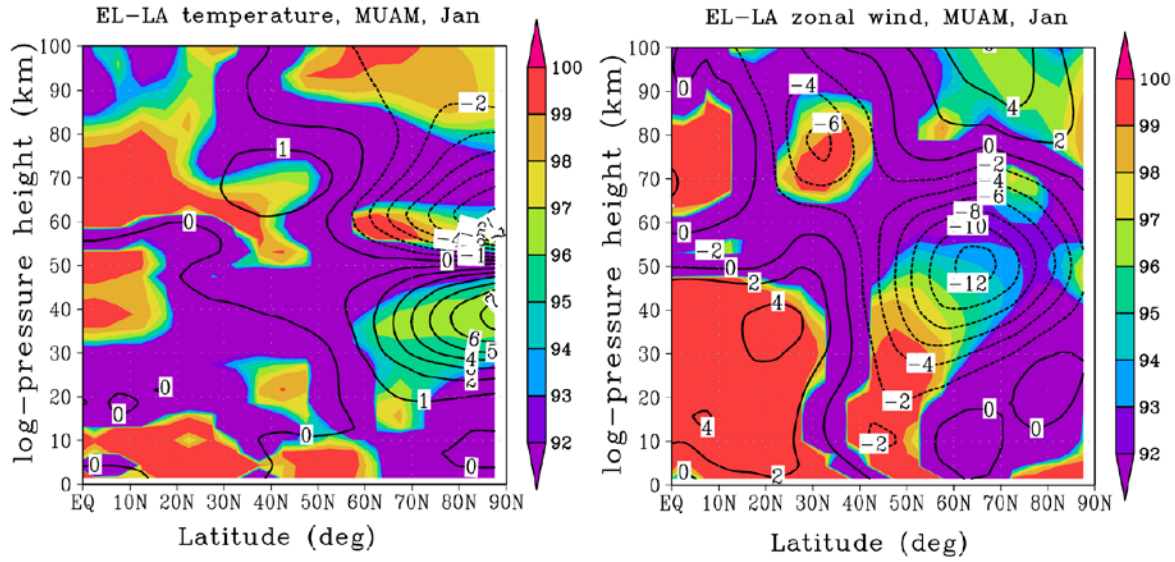

Fig. 4: El Niño – La Niña differences of January mean temperature (left) and zonal wind (right) as simulated with MUAM (contour lines). The colour coding shows the significance of the differences according to a t-test.

5. Conclusions

Radar observations of winds over Collm have shown that the zonal wind in the MLT region in February is correlated with the Eastern Pacific SST. In the upper mesosphere, the effect reduces and there is a tendency that it even reverses, although the effect is not significant at 82 km. Earlier reports on El Niño effects on the MLT often has used observations at about 90 km (e.g. Jacobi, 2009). At this altitude, however, the response of the zonal wind to El Niño is weak (correlation coefficient of about 0.5 in February, see Fig. 2).

The decrease of the correlation in the upper mesosphere is in correspondence with MUAM model analyses that show that the negative zonal wind response in the stratosphere and mesosphere is reversed in the MLT.

Acknowledgements

Niño3 indices based on NOAA ERSST.v4 seas surface temperatures have been kindly provided by KNMI through the KNMI climate explorer, https://climexp.knmi.nl. Ch. Jacobi and D. Mewes acknowledge support by the SFB/TR 172 in Project D01 funded by the Deutsche Forschungsgemeinschaft (DFG). MUAM model simulations were supported by the Russian Science Foundation through grant number 14-17-00685.

6. References

Camp, C.D., Tung, K.-K., 2007: Stratospheric polar warming by ENSO in winter: A statistical study, Geophys. Res. Lett., 34, L04809, doi:10.1029/2006GL028521.

Cullather, R.I., Lim, Y.-K., Boisvert, L.N., Brucker, L., Lee, J.N., Nowicki, S.M.J., 2016: Analysis of the warmest Arctic winter, 2015–2016, Geophys. Res. Lett., 43, 10,808–10,816, doi:10.1002/2016GL071228.

Fischer, A.M., Shindell, D. T., Winter, B., Bourqui, M.S., Faluvegi, G., Rozanov, E., Schraner, M., Brönnimann, S., 2008: Stratospheric winter climate response to ENSO in three chemistry-climate models, Geophys. Res. Lett., 35, L13819, doi:10.1029/2008GL034289.

Fomichev, V.I., Shved, G.M., 1985: Parameterization of the radiative flux divergence in the 9.6 μm O3 band, J. Atmos. Terr. Phys. 47, 1037-1049, doi:10.1016/0021-9169(85)90021-2.

Fomichev, V.I., Blanchet, J.-P. , Turner, D.S., 1998: Matrix parameterization of the 15 μm CO2 band cooling in the middle and upper atmosphere for variable CO2 concentration, J. Geophys. Res. 103(D10), 11505–11528, doi: 10.1029/98JD00799.

Fröhlich, K., Pogoreltsev, A., Jacobi, Ch., 2003: The 48 Layer COMMA-LIM Model: Model description, new aspects, and Climatology, Rep. Inst. Meteorol. Univ. Leipzig, 30, 157-185.

Garcia-Herrera, R., Calvo, N., Garcia, R.R., Giorgetta M.A., 2006: Propagation of ENSO temperature signals into the middle atmosphere: A comparison of two general circulation models and ERA-40 reanalysis data, J. Geophys. Res., 111, D06101, doi:10.1029/2005JD006061.

Hocking, W.K., Fuller, B., Vandepeer, B., 2001: Real-time determination of meteor-related parameters utilizing modern digital technology, J. Atmos. Sol.-Terr. Phys., 63, 155-169, doi: 10.1016/S1364-6826(00)00138-3.

Huang, B., Banzon, V.F., Freeman, E., Lawrimore, J., Liu, W., Peterson, T.C., Smith, T.M., Thorne, P.W., Woodruff, S.D., Zhang H.-M., 2015: Extended Reconstructed Sea Surface Temperature version 4 (ERSST.v4): Part I. Upgrades and intercomparisons, J. Clim., 28. 911-930, doi:10.1175/JCLI-D-14-00006.1.

Jacobi Ch., 2009: Possible signal of tropospheric circulation patterns in middle atmosphere dynamics, Collm (51.3°N, 13°E) mesosphere lower thermosphere winds 1979-2008, Rep. Inst. Meteorol. Univ. Leipzig, 45, 153-162.

Jacobi, Ch., Kürschner, D., 2002: A possible connection of midlatitude mesosphere/lower thermosphere zonal winds and the Southern Oscillation, Phys. Chem. Earth, 27, 571-577, doi:10.1016/S1474-7065(02)00039-6.

Jacobi, Ch., 2012: 6 year mean prevailing winds and tides measured by VHF meteor radar over Collm (51.3°N, 13.0°E), J. Atmos. Sol.-Terr. Phys., 78–79, 8–18, doi:10.1016/j.jastp.2011.04.010.

Jacobi, Ch., Ermakova, T., Mewes, D., Pogoreltsev, A.I., 2017: El Niño influence on the mesosphere/lower thermosphere circulation at midlatitudes as seen by a VHF meteor radar at Collm (51.3oN, 13oE), Adv. Radio Sci., 15, 1–8, doi:10.5194/ars-15-1-2017.

Kennedy, J., Morice, C., Parker, D. Kendon, M., 2016: Global and regional climate in 2015. Weather, 71, 185–192. doi:10.1002/wea.2760

KNMI: KNMI climate explorer, https://climexp.knmi.nl, downloaded 27.5.2016.

Kobayashi, S., Ota, Y., Harada, Y., Ebita, A., Moriya, M., Onoda, H., Onogi, K., Kamahori, H., Kobayashi, C., Endo, H., Miyaoka, K., Takahashi, K., 2015: The JRA-55 Reanalysis: General specifications and basic characteristics, J. Meteorol. Soc. Japan, 93, 5-48, doi: 10.2151/jmsj.2015-001.

Li, T., Calvo, N., Yue, J., Dou, X., Russell III, J.M., Mlynczak, M.G., She, C.-Y., Xue, X., 2013: Influence of El Niño-Southern Oscillation in the mesosphere, Geophys. Res. Lett., 40, 3292–3296, doi:10.1002/grl.50598.

Lu, C., Liu, Y., Liu, C., 2011: Middle atmosphere response to ENSO events in Northern Hemisphere winter by the Whole Atmosphere Community Climate Model, Atmosphere-Ocean, 49:2, 95-111, DOI: 10.1080/07055900.2011.576451.

Pogoreltsev, A.I., Vlasov, A.A., Fröhlich, K., Jacobi, Ch., 2007: Planetary waves in coupling the lower and upper atmosphere, J. Atmos. Sol.-Terr. Phys., 69, 2083–2101, doi:10.1016/j.jastp.2007.05.014.

Polvani., L.M., Sun, L., Butler, A.H., Richter, J.H.,Deser, C., 2017: Distinguishing stratospheric sudden warmings from ENSO as key drivers of wintertime climate variability over the North Atlantic and Eurasia

Portnyagin, Yu., T. Solovjova, T., Merzlyakov, E., Forbes, J., Palo, S., Ortland, D., Hocking, W., MacDougall, J., Thayaparan, T., Manson, A., Meek, C., Hoffmann, P., Singer, W., Mitchell, N., Pancheva, D., Igarashi, K., Murayama, Y., Jacobi, Ch.,

Kürschner, D., Fahrutdinova, A., Korotyshkin, D., Clark, R., Tailor, M., Franke, S., Fritts, D., Tsuda, T., Nakamura, T., Gurubaran, S., Rajaram, R., Vincent, R., Kovalam, S., Batista, P., Poole, G., Malinga, S., Fraser, G., Murphy, D., Riggin, D., Aso, T., Tsutsumi, M., 2004: Mesosphere/lower thermosphere prevailing wind model, Adv. Space Res., 34, 1755-1762, doi:10.1016/j.asr.2003.04.058.

Rienecker, M.M., Suarez, M.J., Gelaro, R., Todling, R., Bacmeister, J., Liu, E., Bosilovich, M. G., Schubert, S. D., Takacs, L., Kim, G.-K., Bloom, S., Chen, J., Collins, D., Conaty, A. da Silva, A., et al., 2011: MERRA: NASA's Modern-Era Retrospective Analysis for Research and Applications, J. Clim., 24, 3624-3648, doi:10.1175/JCLI-D-11-00015.1.

Stober, G., Jacobi, Ch., Fröhlich, K., Oberheide, J., 2008: Meteor radar temperatures over Collm (51.3°N, 13°E), Adv. Space Res., 42, 1253-1258, doi:10.1016/j.asr.2007.10.018.

Swinbank, R., Ortland, D.A., 2003: Compilation of wind data for the Upper Atmosphere Research Satellite (UARS) Reference Atmosphere Project, J. Geophys. Res., 108, 4615, doi:10.1029/2002JD003135.

Taguchi, M., and Hartmann, D.L., 2006: Increased occurrence of stratospheric sudden warmings during El Niño as simulated by WACCM, J. Clim., 19, 324–332, doi:10.1175/jcli3655.1.

Trenberth, K. E., 1997: The definition of El Niño, Bull. Am. Meteorol. Soc., 78, 2771–2777, doi: 10.1175/1520-0477(1997)078<2771:TDOENO>2.0.CO;2.